

point mutations on the performance of digital organisms. In all cases, the fitness (replication rate) of each mutant was calculated in the same environment in which its simple or complex parent evolved, and the mutant's fitness is expressed relative to the parent. The first tool makes every possible one-step point mutant for a particular parent. The default set includes 28 different instructions; given a parent of genome length 80, for example, there are $80 \times (28 - 1) = 2,160$ different one-step point mutants. The mean fitness of these mutants permits exact calculation of α in the decay test. The second tool produces a random sample of progeny that differ from their parent by two or more point mutations. For each parent, we generated between 10^5 and 10^7 progeny with two mutations, three mutations and so on, up to ten mutations. The third tool produces and analyses pairs of point mutations alone and in combination; for each two-step mutant, we have both corresponding one-step mutants. Having the single mutants allows us to compare a double mutant's actual fitness with the exact value expected under the hypothesis that the mutations interact in a multiplicative manner. We ran the pair test on 10^4 and 10^5 mutational pairs for each complex and simple organism, respectively.

Statistical methods. We performed the Wilcoxon signed-ranks test on the difference scores for all comparisons between complex and simple organisms²⁹. This test reflects the evolutionary relationship between pairs of organisms; it is also non-parametric and thus insensitive to deviations from a normal distribution. To estimate β in the decay tests, we minimized the sum of squared deviations around the log-transformed mean fitness values. We excluded samples with fewer than 100 viable mutants, in which case log mean fitness was poorly estimated. By increasing sample size to 10^8 , we can obtain additional viable mutants; the exclusion of some values because of insufficient sampling appears to have no systematic effect on estimation of β .

Received 12 April; accepted 27 May 1999.

1. Ray, T. S. in *Artificial Life II* (eds Langton, C. G., Taylor, C., Farmer, J. D. & Rasmussen, S.) 371–408 (Addison-Wesley, Redwood City, California, 1991).
2. Adami, C. Learning and complexity in genetic auto-adaptive systems. *Physica D* **80**, 154–170 (1995).
3. Adami, C. *Introduction to Artificial Life* (Springer, New York, 1998).
4. Elena, S. F. & Lenski, R. E. Test of synergistic interactions among deleterious mutations in bacteria. *Nature* **390**, 395–398 (1997).
5. De Visser, J. A. G. M., Hoekstra, R. F. & van den Ende, H. Test of interaction between genetic markers that affect fitness in *Aspergillus niger*. *Evolution* **51**, 1499–1505 (1997).
6. Clark, A. G. & Wang, L. Epistasis in measured genotypes: *Drosophila* P-element insertions. *Genetics* **147**, 157–163 (1997).
7. Wright, S. *Evolution and the Genetics of Populations* (Univ. Chicago Press, 1977).
8. Kauffman, S. & Levin, S. Towards a general theory of adaptive walks on rugged landscapes. *J. Theor. Biol.* **128**, 11–45 (1987).
9. Kauffman, S. A. *The Origins of Order* (Oxford Univ. Press, New York, 1993).
10. Paquin, C. & Adams, J. Relative fitness can decrease in evolving populations of *S. cerevisiae*. *Nature* **306**, 368–371 (1983).
11. Dykhuizen, D. E., Dean, A. M. & Hartl, D. L. Metabolic flux and fitness. *Genetics* **115**, 25–31 (1987).
12. Lenski, R. E. & Travisano, M. Dynamics of adaptation and diversification: a 10,000-generation experiment with bacterial populations. *Proc. Natl Acad. Sci. USA* **91**, 6808–6814 (1994).
13. Rosenzweig, R. F., Sharp, R. R., Treeves, D. S. & Adams, J. Microbial evolution in a simple unstructured environment: genetic differentiation in *Escherichia coli*. *Genetics* **137**, 903–917 (1994).
14. Travisano, M., Mongold, J. A., Bennett, A. F. & Lenski, R. E. Experimental tests of the roles of adaptation, chance, and history in evolution. *Science* **267**, 87–90 (1995).
15. Rainey, P. B. & Travisano, M. Adaptive radiation in a heterogeneous environment. *Nature* **394**, 69–72 (1998).
16. Burch, C. L. & Chao, L. Evolution by small steps and rugged landscapes in the RNA virus $\phi 6$. *Genetics* **151**, 921–927 (1999).
17. De Visser, J. A., Zeyl, C. W., Gerrish, P. J., Blanchard, J. L. & Lenski, R. E. Diminishing returns from mutation supply rate in asexual populations. *Science* **283**, 404–406 (1999).
18. Turner, P. E. & Chao, L. Prisoner's dilemma in an RNA virus. *Nature* **398**, 441–443 (1999).
19. Maynard Smith, J. Byte-sized evolution. *Nature* **335**, 772–773 (1992).
20. Holland, J. H. *Adaptation in Natural and Artificial Systems* (MIT Press, Cambridge, Massachusetts, 1992).
21. Koza, J. R. *Genetic Programming* (MIT Press, Cambridge, Massachusetts, 1992).
22. Frank, S. A. in *Adaptation* (eds Rose, M. R. & Lauder, G. V.) 451–505 (Academic, New York, 1996).
23. Koza, J. R., Bennett, F. H., Andre, D. & Keane, M. A. in *Evolutionary Robotics* (ed. Gomi, T.) 37–76 (AAI Press, Kanata, Canada, 1998).
24. Maynard Smith, J. *The Evolution of Sex* (Cambridge Univ. Press, 1978).
25. Kondrashov, A. S. Deleterious mutations and the evolution of sexual reproduction. *Nature* **336**, 435–440 (1988).
26. Hurst, L. D. & Peck, J. R. Recent advances in understanding of the evolution and maintenance of sex. *Trends Ecol. Evol.* **11**, 46–52 (1996).
27. Otto, S. P. & Feldman, M. W. Deleterious mutations, variable epistatic interactions, and the evolution of recombination. *Theor. Popul. Biol.* **51**, 134–147 (1997).
28. Eyre-Walker, A. & Keightley, P. D. High genomic deleterious mutation rates in hominids. *Nature* **397**, 344–347 (1999).
29. Sokal, R. R. & Rohlf, F. J. *Biometry* 3rd edn (Freeman, New York, 1994).

Acknowledgements. We thank A. De Visser, S. Elena, D. Lenski, P. Moore, A. Moya and S. Remold for comments, discussion and technical assistance. Access to a Beowulf system was provided by the Center for Advanced Computing Research at the California Institute of Technology. This work was supported by an NSF grant to C.A. and a fellowship from the MacArthur Foundation to R.E.L.

Correspondence should be addressed to R.E.L. (e-mail: lenski@pilot.msu.edu); requests for materials to C.O. (e-mail: charles@krl.caltech.edu) or see <http://www.krl.caltech.edu/avida/pubs/nature> 99.

A general model for the structure and allometry of plant vascular systems

Geoffrey B. West^{*†}, James H. Brown^{†‡} & Brian J. Enquist^{†‡}

^{*} Theoretical Division, T-8, MS B285, Los Alamos National Laboratory, Los Alamos, New Mexico 87545, USA

[†] The Santa Fe Institute, 1399 Hyde Park Road, Santa Fe, New Mexico 87501, USA

[‡] Department of Biology, University of New Mexico, Albuquerque, New Mexico 87131, USA

Vascular plants vary in size by about twelve orders of magnitude, and a single individual sequoia spans nearly this entire range as it grows from a seedling to a mature tree. Size influences nearly all of the structural, functional and ecological characteristics of organisms^{1,2}. Here we present an integrated model for the hydrodynamics, biomechanics and branching geometry of plants, based on the application of a general theory of resource distribution through hierarchical branching networks³ to the case of vascular plants. The model successfully predicts a fractal-like architecture and many known scaling laws, both between and within individual plants, including allometric exponents which are simple multiples of 1/4. We show that conducting tubes must taper

Box 1 Notation and geometry

The model can be described as a continuously branching hierarchical network running from the trunk (level 0) to the petioles (level N), with an arbitrary level denoted by k (Fig. 1). The architecture is characterized by three parameters (\bar{a} , $\bar{\alpha}$ and n), which relate daughter to parent branches: ratios of branch radii, $\beta_k \equiv r_{k+1}/r_k \equiv n^{-\bar{\alpha}/2}$, tube radii, $\tilde{\beta}_k \equiv a_{k+1}/a_k \equiv n^{-\bar{\alpha}/2}$, and branch lengths, $\gamma_k \equiv l_{k+1}/l_k$ and also the branching ratio, n , the number of daughter branches derived from a parent branch. Because the total number of tubes is preserved at each branching, $n = n_{k+1}/n_k$, where n_k is the number of tubes in a k th-level branch; n is taken to be independent of k and typically equals 2. Clearly, $n_k = n_N n^{N-k}$, where N is the total number of branching generations from trunk to petiole, and n_N is the number of tubes in a petiole, which is taken to be an invariant. Now, for a volume-filling network, $\gamma_k = n^{-1/3}$, independent of k (ref. 3). If tube tapering is uniform, $\bar{\alpha}$ is also independent of k , and it follows that

$$\frac{r_k}{r_N} = n^{(N-k)\bar{\alpha}/2}; \quad \frac{a_k}{a_N} = \left(\frac{r_k}{r_N}\right)^{\bar{\alpha}/\bar{a}}; \quad \frac{l_k}{l_N} = \left(\frac{r_k}{r_N}\right)^{2/\bar{a}\bar{\alpha}} \quad (1)$$

Various scaling laws can now be derived. For example, the number of terminal branches or leaves distal to the k th branch, $n_k^t \equiv n_k/n_N = n^{N-k} = (r_k/r_N)^{2\bar{a}}$, and the area of conductive tissue (CT), $A_k^{CT} \equiv n_k \pi \bar{a}_k^2 = A_N^{CT} (r_k/r_N)^{2(1+\bar{a})/\bar{a}}$, where $A_N^{CT} \equiv n_N \pi \bar{a}_N^2$ is the area of conductive tissue in a petiole. Thus, the area of conductive tissue relative to the total (tot) branch cross-sectional area ($A_k^{\text{tot}} \equiv \pi r_k^2$) is given by

$$f_k \equiv \frac{A_k^{CT}}{A_k^{\text{tot}}} = n_N \left(\frac{\bar{a}_N}{r_N}\right)^2 \left(\frac{r_k}{r_N}\right)^{2(1+\bar{a})/\bar{a}\bar{\alpha}} \quad (2)$$

The total cross-sectional area scales as $n A_{k+1}^{\text{tot}}/A_k^{\text{tot}} \equiv n \beta_k^2 \equiv n^{1-\bar{a}}$. When $\bar{a} = 1$ this reduces to unity and the branching is area-preserving; that is, the cross-sectional area of the daughter branches is equal to that of the parent: $n A_{k+1}^{\text{tot}} = A_k^{\text{tot}}$. A simple example of this, considered in ref. 3, is the pipe model⁶, in which all tubes have the same constant diameter ($\bar{a} = 0$), are tightly bundled and have no non-conducting tissue. Here we consider the more realistic case in which tubes are loosely packed in sapwood and there may be non-conducting heartwood providing additional mechanical stability.

and, consequently, that the resistance and fluid flow per tube are independent of the total path length and plant size. This resolves the problem of resistance increasing with length, thereby allowing plants to evolve vertical architectures and explaining why the maximum height of trees is about 100 m. It also explains why the energy use of plants in ecosystems is size independent.

Most size-related variation can be characterized by allometric scaling laws of the form $Y = Y_0 M^b$, where Y is the variable of interest, Y_0 is a normalization constant, M is body mass and b is the scaling exponent. Although an enormous amount of anatomical and physiological data exist for plants^{2,4-17}, no single model has explained these diverse phenomena. We have modelled the transport of fluid from the trunk to the petioles through the xylem vessels of angiosperms (flowering plants). The model is based on a few general principles: (1) the branching network is volume filling; (2) the leaf and petiole size are invariant; (3) biomechanical constraints are uniform; and (4) energy dissipated in fluid flow is minimized. The model should also apply, with only minor modification, to transport through tracheids, phloem and roots.

The network is assumed to be composed of identical tubes of equal length running continuously in parallel from trunk to petiole (files of vessels connected in series). Tube diameter is taken to be constant within a branch segment but is allowed to vary between segments, thereby incorporating possible tapering. For simplicity, tapering within segments is ignored, as are the thickness and structure of the tube walls and connections between tubes. The notation and geometry of the model are described in Box 1, where it is shown that scaling relations can be parametrized in terms of just two exponents, a and \bar{a} , which determine how radii of branches and tubes scale within a plant. Box 2 shows how \bar{a} , and consequently the degree of tapering, are determined from hydrodynamic considerations, whereas a is determined from mechanical constraints.

The design of trunks and branches to resist buckling leads to some optimal relationship between their length and radius: $l_k \propto r_k^\alpha$. Comparison with equation (1) in Box 1 gives $a = 2/(3\alpha)$. If this holds uniformly for all branches, then α is constant, independent of k , in which case a and β_k are also constant. When coupled with the volume-filling constraint, $\gamma_k = n^{-1/3}$, this proves that the branching

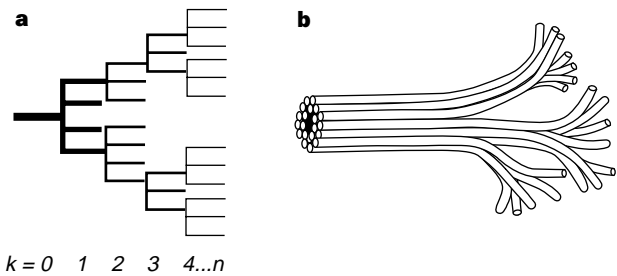


Figure 1 Branching structure. **a**, Topology of a plant branching network. **b**, Symbolic representation of branch vascular structure, showing conducting tubes and non-conducting tissue (black).

architecture is a self-similar fractal^{18,19}. Analyses based on solutions to the bending moment equations for beams give $\alpha = 2/3$ (refs 2, 20). This is most important for the trunk and large branches^{7,15,20}. Assuming that it holds for all branches (all k) leads to $a = 1$, which is the condition for area-preserving branching³. Unlike a previous report³, this derivation does not assume the pipe model. The result $a = 1$ implies that the leaf area distal to the k th branch $A_k^L = C_L r_k^2$, where $C_L \equiv a_L/r_N^2$ is invariant, a_L is the average area of a leaf, and r_N is the radius of a petiole. Taking $r_N \approx 0.5$ mm and $a_L \approx 30$ cm² gives $C_L \approx 1.2 \times 10^4$. The number of branches of a given size $N_k = n^k = n^N (r_N/r_k)^2 \propto r_k^{-2}$ (refs 2, 4, 6, 8, 12). These results are independent of \bar{a} .

The linear increase in hydrodynamic resistance with length implied by the classic Poiseuille formula⁴ for a uniform tube would preclude the very existence of tall trees, regardless of any mechanical constraint; for example, lower branches would be favoured over branches in the upper canopy where most light is collected. However, as shown in Box 2, if tubes taper, their total resistance from trunk to petiole Z_i need not increase with their total length. Indeed, for $\bar{a} > 1/6$, Z_i is a constant independent of total tube length and is the same for all plants, regardless of size. This ensures an equal supply to all leaves, both at different heights within a plant, and in plants of different sizes growing in similar environments. To avoid excess tapering, \bar{a} should be the minimum possible value consistent with constant Z_i , namely $1/6$.

Box 3 shows how general scaling relationships for various physical quantities are derived in terms of a and \bar{a} . We now consider some consequences in the idealized case, where $a = 1$ (the area-preserving branching condition derived from biomechanical constraints) and $\bar{a} = 1/6$ (derived from minimizing tapering and hydrodynamic resistance).

Box 2 Hydrodynamics and vessel tapering

The resistance, Z_k , of a single tube (i) within any branch segment (k) is given by the Poiseuille formula⁴ ($Z_k = 8\eta l_k / \pi r_k^4$), where η is the fluid viscosity. The total resistance of a tube running from the trunk to a petiole through successive branch segments is $Z_i = \sum_{k=0}^N Z_k$. Using equation (1), this can be expressed as

$$Z_i = \sum_{k=0}^N Z_k = \left[\frac{1 - [(n^{1/3} - 1)l_T/l_N]^{(1-\bar{a}n)}}{1 - n^{(1/3-2\bar{a})}} \right] Z_N \quad (3)$$

where $Z_N = 8\eta l_N / \pi a_N^4$ is the resistance of a tube in the petiole, and the total tube length $l_T = \sum_{k=0}^N l_k = l_0 / (1 - n^{-1/3})$. The crucial point is that, when $l_T \gg l_N$, the behaviour of Z_i depends critically on the degree of tapering, that is, whether \bar{a} is less than, more than, or equal to $1/6$. First, consider $\bar{a} < 1/6$, which includes the pipe model; then equation (3) gives $Z_i \propto (l_T/l_N)^{(1-\bar{a}n)}$, so resistance increases with path length, l_T . However, if $\bar{a} > 1/6$, then $Z_i \approx Z_N / [1 - n^{(1/3-2\bar{a})}]$, which can be shown to be its minimum value. This has the remarkable property that it is a constant, independent of total tube length, l_T , because Z_N is an invariant, Z_i is also the same for all plants, regardless of size. Taking $\bar{a} \rightarrow 1/6$ to minimize tapering, yet keeping Z_i constant, gives $\bar{a} \approx 1/6 + (2N \ln n)^{-1}$. Thus, for large N (tall trees), $\bar{a} \approx 1/6$; for example, with $r_0 \approx 25$ cm and $N \approx 20$, the correction is only $\sim 1/30$. For small trees, however, whose height $h \ll e^{(6\bar{a}-1)^{-1}} l_N / (n^{1/3} - 1) \approx$ a few metres, the correction can be large, leading to calculable deviations from results derived using $\bar{a} = 1/6$. At this precise value, Z_i increases logarithmically with l_T , so \bar{a} should implicitly be taken as infinitesimally larger than $1/6$.

Box 3 Scaling relations and allometry

Scaling relations within an individual plant are easily derived. Here we present some general formulae expressed in terms of a and \bar{a} . Because tubes are in parallel, the resistance of a branch segment is given by $Z_k = Z_i / n_k = 8\eta l_k / \pi n_k r_k^4$ and its conductivity by $K_k = l_k / Z_k = K_N (r_k/r_N)^{2(1+2\bar{a})/a}$, where $K_N = \pi n_N a_N^4 / 8\eta$ is the conductivity of a petiole. Similarly, leaf-specific conductivity (the conductivity per unit leaf area), $L_k = K_k / n_k^L a_L = L_N (r_k/r_N)^{4\bar{a}/a}$. Alternatively, these can be expressed as a function of the area of conducting tissue: $K_k \propto (A_k^{\text{CT}})^{(1+2\bar{a})/(1+\bar{a})}$ and $L_k \propto (A_k^{\text{CT}})^{(2\bar{a})/(1+\bar{a})}$ (refs 8-10).

Allometric relations can be derived by considering the total wood volume, V_W , which, for constant density, is proportional to the total mass, M . Thus, $V_W = \sum_{k=0}^N \pi n_k^L r_k^2 l_k = (\gamma \beta^2)^{-N} V_N / [1 - n \gamma \beta^2]$, where $\gamma = n^{-1/3}$, $\beta = n^{-a/2}$ and V_N is the volume of a petiole. Consequently, the total number of terminal branches, or leaves, should scale as $n_0^L = n^N \propto M^{3/(1+3\bar{a})}$. Similarly, from equation (1), $l_k \propto M^{(1-k)/(N(a+3))}$ and $r_k \propto M^{(1-k/N)(3a/2(a+3))}$, so the length and radius of a k th-level branch scale more slowly with M than those of the trunk, which scale as $l_0 \propto M^{1/(a+3)}$, and $r_0 \propto M^{3a/(2(a+3))}$.

First, the conductivity of a branch segment scales as $K_k/K_N \propto (r_k/r_N)^{8/3} \propto (A_k^{CT})^{8/7}$ and its leaf-specific conductivity as $L_k/L_N \propto (r_k/r_N)^{2/3} \propto (A_k^{CT})^{2/7}$. For a petiole with $a_N \approx 10 \mu\text{m}$ and $n_N \approx 200$, its conductivity $K_N \approx 7 \times 10^{-10} \text{ m}^4 \text{ s}^{-1} \text{ MPa}^{-1}$. For comparison, the pipe model, where $a = 1$ and $\bar{a} = 0$, incorrectly gives $K_k \propto r_k^2$ and $L_k \propto r_k^0$.

Second, the total number of terminal branches or leaves scales as $n_0^I = n^N \propto r_0^2 \propto M^{3/4}$. Similarly, the length and radius of the trunk scale as $l_0 \propto M^{1/4}$ and $r_0 \propto M^{3/8}$, respectively². The total height of a tree, h , is equivalent to the length of a tube running from trunk to leaf: $h = l_T \approx l_0/(1 - \gamma)$, so $h \propto M^{1/4}$. The number of branching generations, N , grows only logarithmically with mass, $N \propto \ln M$, and can be estimated from $N = 2\ln(r_0/r_N)/\ln n$. For a tree with trunk diameter 50 cm, petiole radius 0.5 mm and $n = 2$, this gives $N \approx 18$. From equation (1), the tube radius scales as $a_k/a_N = (r_k/r_N)^{1/6} \propto M^{(1-k/N)/16}$, so, in the trunk relative to the petiole, $a_0/a_N = n^{N/12} \propto M^{1/16}$. Taking $N \approx 18$ and $n = 2$, this gives $a_0/a_N \approx 2.8$, so, if $a_N \approx 10 \mu\text{m}$, then $a_0 \approx 30 \mu\text{m}$. Furthermore, over variation in mass of 12 orders of magnitude, the radius of a xylem vessel in the trunk, a_0 , should change by only about 60% (refs 4, 11).

Third, the pressure gradient across an arbitrary branch, $\Delta P_k/l_k$ scales as $l_k^{-6\bar{a}} = l_k^{-1}$ and so is steeper in smaller branches than larger ones. In particular, the ratio between trunk and petiole is predicted to be $(\Delta P_0/l_0)/(\Delta P_N/l_N) = l_N/l_0 \propto M^{-1/4}$, and so is smaller in taller trees. If $l_0 \approx 4 \text{ m}$ and $l_N \approx 4 \text{ cm}$, then this ratio is $\sim 1/100$ (refs 4, 5). The flow rate through a single tube $\dot{Q}_i = \Delta P/Z_i$, where ΔP is the overall pressure difference between air and soil. Because Z_i and ΔP are both independent of plant size, \dot{Q}_i must also be size independent; the flow rate in a tube in a large tree is therefore the same as that in a small plant. This is the origin of the 'energy equivalence relationship'²¹. Metabolic rate, B , the rate of gross photosynthesis, is proportional to the total volume flow rate through all n_0 vascular tubes, and is therefore given by $\dot{Q}_0 = n_0 \dot{Q}_i = n^N n_N \dot{Q}_i \propto M^{3/4}$ (refs 2, 21). Thus $B \propto M^{3/4}$.

Fourth, tubes taper, so fluid velocity, u_k , must increase in small branches. The flow rate through a single tube is $\dot{Q}_i = \pi a_k^2 u_k$, so $u_k \propto a_k^{-2} \propto r_k^{-1/3}$. Thus, the ratio of petiole to trunk velocities $u_N/u_0 = (r_0/r_N)^{1/3}$. Taking $r_N \approx 0.5 \text{ mm}$ and $r_0 \approx 50 \text{ cm}$ gives $u_N/u_0 \approx 4.6$. Allometrically, u_k scales as $M^{-(1-k/N)/8}$ so, for the trunk, $u_0 \propto M^{-1/8}$. Thus, over eight orders of magnitude variation in mass (roughly a 50-cm sapling relative to a 50-m tree), fluid velocity in the trunk is predicted to decrease by a factor of ~ 10 (ref. 4).

Fifth, a particularly sensitive test of the model is its accurate prediction of how total plant resistance changes as progressively larger branch segments are removed (Box 4).

Finally, if tapering continued indefinitely, vessel radii in the trunk would become too large, leading to a maximum height for trees. In Box 5 we show that $h^{\text{max}} \sim 100 \text{ m}$.

Although the model makes several simplifying assumptions, its power rests on fundamental physical and biological principles as well as realistic features of the architecture, biomechanics and hydrodynamics of vascular plants. It accurately predicts scaling exponents (Table 1), their normalizations and the magnitude of

Box 4 Removing branch segments

Suppose that only branches up to the k th level remain. Because the total number of tubes in the trunk is still n_0 , the total resistance of the remaining branch network is $Z_k^{\text{TOT}} = (\sum_{i=k}^N Z_i^k)/n_0$; note that Z_N^{TOT} is the total resistance of the uncut tree. The ratio of these, $R_k \equiv Z_k^{\text{TOT}}/Z_N^{\text{TOT}}$, is given by $R_k = [(r_{k+1}/r_0)^p - 1]/[(r_{N+1}/r_0)^p - 1]$, where $p \equiv 2(1 - 6\bar{a})/3a$ and $r_{N+1} \equiv r_N n^{-a/2}$. Note that $R_N = 1$ and $R_{-1} = 0$, the latter corresponding to the limit where all conducting tissue has been removed. As shown in Fig. 2, our prediction, $\bar{a} = 1/6$, agrees very well with measured values¹² and provides a much better fit than the classic pipe model, $\bar{a} = 0$.

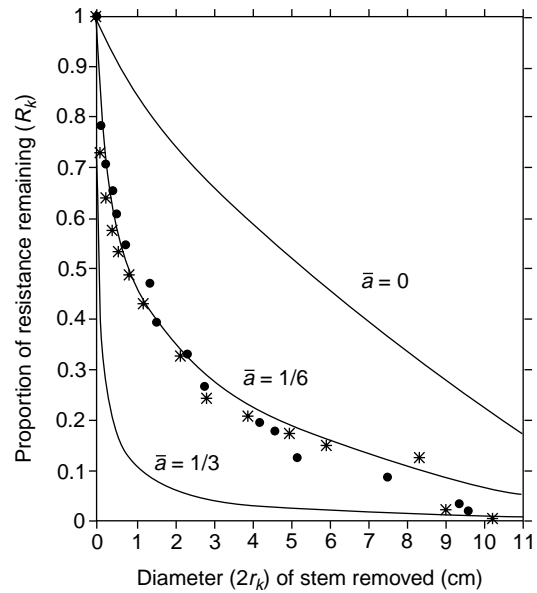


Figure 2 Effect of sequentially removing branches of increasing radius, r_k , on the proportion of total resistance remaining, R_k . The predicted value, $\bar{a} = 1/6$, is in excellent agreement with the data¹² that represent two trees. In contrast, $\bar{a} = 0$, corresponding to no tapering of tubes as in the pipe model⁶, and $\bar{a} = 1/3$, give poor agreement. The curves terminate when only the trunk remains. If extrapolated, all would converge at the trunk diameter, $\sim 14.5 \text{ cm}$, where $r_k = r_0$ and no conducting tissue remains, such that $R_k = R_1 = 0$.

many variables such as leaf area supplied by a tube and conductivity of a branch segment^{8,10-12}. We are unaware of any data that seriously disagree with its predictions. Because this zeroth-order model describes an 'average idealized' plant, it can serve as a starting point for more elaborate models that incorporate special features of plants of different taxa or growing in different environments. Such complications include: (1) variation in vessel size within and among plants growing in different environments; (2) horizontal flow between parallel tubes; (3) variation in tube length and branching symmetry (but see ref. 22); (4) variation in α , that is, not all branches are subject to the same biomechanical constraint^{2,15}; (5) departures from precise volume filling in plants such as palms, vines,

Box 5 Area of conducting tissue and the maximum height of trees

From the argument leading to equation (2), we have $A_k^{CT} \propto r_k^{2(1+\bar{a})/6} \propto A_N^{\text{TOT}7/6}$. This can be expressed in terms of the number of leaves, n_k^L , distal to the k th level branch: $A_k^{CT} \propto (n_k^L)^{1+\bar{a}} \propto (n_k^L)^{7/6}$. Now, from equation (2), the proportion of conductive tissue relative to total cross-sectional area of a branch scales as $f_k \propto r_k^{2(1+\bar{a})-6\bar{a}} \propto r_k^{1/3}$ (refs 8, 13, 14). For the trunk, in particular, we necessarily have $f_0 \leq 1$, so equation (2) leads to a limitation on the radius and consequently the height of a tree:

$$h^{\text{max}} = \frac{l_N}{(1-n^{-1/3})} \left(\frac{r_N^2}{a_N^2 n_N} \right)^{1/3(1+\bar{a}-a)} ; r_0^{\text{max}} = r_N \left(\frac{r_N^2}{a_N^2 n_N} \right)^{a/2(1+\bar{a}-a)}$$

With $a = 1$ and $\bar{a} = 1/6$, $h^{\text{max}} = l_N n_N^4 / [a_N^4 n_N^2 (1 - n^{-1/3})]$ and $r_0^{\text{max}} = r_N^7 / [a_N^6 n_N^3]$. Because of the large exponents, these formulae are very sensitive to the parameters of the petiole. For example, take $r_N = 0.5 \text{ mm}$, $a_N = 10 \mu\text{m}$, and $n_N = 200$, then $r_0^{\text{max}} \approx 1 \text{ m}$ and $h^{\text{max}} \approx 40 \text{ m}$; if, instead, $a_N = 8 \mu\text{m}$, then $r_0^{\text{max}} \approx 4 \text{ m}$ and $h^{\text{max}} \approx 100 \text{ m}$. Thus, although these formulae cannot be used to accurately estimate maximum size, they do show why h^{max} is of the order of 100 m rather than 1 m or 1,000 m. This provides a fundamental mechanical and hydrodynamic explanation why the size of trees is limited. If the network were not optimized, then h^{max} would be substantially reduced; for example, if $\bar{a} = 1/3$, then $h^{\text{max}} \approx 1 \text{ m}$. Thus, if trees are to grow tall, \bar{a} must approach the optimal minimum value, $1/6$.

Table 1 Predicted values of scaling exponents for physiological and anatomical variables of plant vascular systems.

Variable	Plant mass		Branch radius		
	Exponent predicted	Symbol	Symbol	Exponent	
				Predicted	Observed
Number of leaves	$\frac{3}{4}$ (0.75)	n_0^l	n_k^l	2 (2.00)	2.007 (ref. 12)
Number of branches	$\frac{3}{4}$ (0.75)	N_0	N_k	-2 (-2.00)	-2.00 (ref. 6)
Number of tubes	$\frac{3}{4}$ (0.75)	n_0	n_k	2 (2.00)	n.d.
Branch length	$\frac{1}{4}$ (0.25)	l_0	l_k	$\frac{2}{3}$ (0.67)	0.652 (ref. 6)
Branch radius	$\frac{3}{8}$ (0.375)	r_0			
Area of conductive tissue	$\frac{7}{8}$ (0.875)	A_0^{CT}	A_k^{CT}	$\frac{7}{3}$ (2.33)	2.13 (ref. 8)
Tube radius	$\frac{1}{16}$ (0.0625)	a_0	a_k	$\frac{1}{6}$ (0.167)	n.d.
Conductivity	1 (1.00)	K_0	K_k	$\frac{8}{3}$ (2.67)	2.63 (ref. 12)
Leaf-specific conductivity	$\frac{1}{4}$ (0.25)	L_0	L_k	$\frac{2}{3}$ (0.67)	0.727 (ref. 17)
Fluid flow rate			\dot{Q}_k	2 (2.00)	n.d.
Metabolic rate	$\frac{3}{4}$ (0.75)	\dot{Q}_0			
Pressure gradient	$-\frac{1}{4}$ (-0.25)	$\Delta P_0/l_0$	$\Delta P_k/l_k$	$-\frac{2}{3}$ (-0.67)	n.d.
Fluid velocity	$-\frac{1}{8}$ (-0.125)	u_0	u_k	$-\frac{1}{3}$ (-0.33)	n.d.
Branch resistance	$-\frac{3}{8}$ (-0.375)	Z_0	Z_k	$-\frac{1}{3}$ (-0.33)	n.d.
Tree height	$\frac{1}{4}$ (0.25)	h			
Reproductive biomass	$\frac{3}{4}$ (0.75)				
Total fluid volume	$\frac{29}{24}$ (1.0415)				

Values are given as a function of total plant mass, M , and branch radius, r_k . For the latter case, predictions are compared with measured values in the last column. References cited do not quote confidence levels, except for branch length, where they are given as ± 0.036 . Because botanists rarely report allometric scaling with mass, no values for observed exponents are quoted. n.d., no data available.

ferns, grasses and saplings with few branches, so that $\gamma \rightarrow n^{-1/2}$ rather than $n^{-1/3}$, leading to $l_k \propto r_k$ (refs 7, 15); and (6) constrictions in tubes at petioles and perhaps at other branch junctions^{4,16}. These complications are expected to have small effects, because many quantities, such as scaling exponents, effectively average out over the whole plant.

The model quantitatively predicts how vessels must taper to compensate for variation in total transport path length. This is supported by measured changes in vessel radius and resistance within and between plants^{4,11} and leads to a maximum height for trees. An important consequence is that tapering ensures comparable xylem flow to all leaves. Competition for light has apparently led to a design that maximizes canopy height and simultaneously minimizes tapering of vascular tubes. In a given environment with a fixed pressure differential between air and soil, on average all xylem tubes of all plants conduct water and nutrients at approximately the same rate. This counterintuitive result provides the fundamental basis for the recently demonstrated equivalence of resource use, independent of plant size, across diverse ecosystems²¹.

The model shows that quarter-power allometric scaling laws, which are well known in animals¹, also apply to many characteristics of plants². There are many parallels: in both, metabolic rate scales as $M^{3/4}$, radius of trunk and aorta as $M^{3/8}$, and size of and fluid velocity in terminal vessels as M^0 . It seems that these scaling laws are nearly universal in biology, and that they have their origins in common geometric and hydrodynamic principles that govern the transport of essential materials to support cellular metabolism. □

Received 27 November 1998; accepted 20 May 1999.

- Schmidt-Nielsen, K. *Scaling: Why is Animal Size so Important?* (Cambridge Univ. Press, Cambridge, 1984).
- Niklas, K. J. *Plant Allometry: The Scaling of Form and Process* (Univ. of Chicago Press, Chicago, 1994).
- West, G. B., Brown, J. H. & Enquist, B. J. A general model for the origin of allometric scaling laws in biology. *Science* **276**, 122–126 (1997).
- Zimmermann, M. H. *Xylem Structure and the Ascent of Sap* (Springer, New York, 1983).
- Tyree, M. T. & Ewers, F. W. The hydraulic architecture of trees and other woody plants. *New Phytol.* **119**, 345–360 (1991).

- Shinozaki, K., Yoda, K., Hozumi, K. & Kira, T. A quantitative analysis of plant form—the pipe model theory: I. Basic analysis. *Jpn. J. Ecol.* **14**, 97–105 (1964).
- Bertram, J. E. A. Size-dependent differential scaling in branches: the mechanical design of trees revisited. *Trees* **4**, 241–253 (1989).
- Patino, S., Tyree, M. T. & Herre, E. A. Comparison of hydraulic architecture of woody plants of differing phylogeny and growth form with special reference to free standing and hemi-epiphytic *Ficus* species from Panama. *New Phytol.* **129**, 125–134 (1995).
- Kuuluvainen, T., Sprugel, D. G. & Brooks, J. R. Hydraulic architecture and structure of *Abies lasiocarpa* seedlings in three alpine meadows of different moisture status in the eastern Olympic mountains, Washington, U.S.A. *Arct. Alp. Res.* **28**, 60–64 (1996).
- Yang, S. & Tyree, M. T. Hydraulic architecture of *Acer saccharum* and *A. rubrum*: comparison of branches to whole trees and the contribution of leaves to hydraulic resistance. *J. Exp. Bot.* **45**, 179–186 (1994).
- Ewers, F. W. & Zimmermann, M. H. The hydraulic architecture of eastern hemlock *Tsuga canadensis*. *Can. J. Bot.* **62**, 940–946 (1984).
- Yang, S. & Tyree, M. T. Hydraulic resistance in *Acer saccharum* shoots and its influence on leaf water potential and transpiration. *Tree Physiol.* **12**, 231–242 (1993).
- Long, J. N., Smith, F. W. & Scott, D. R. M. The role of Douglas fir stem sapwood and heartwood in the mechanical and physiological support of crowns and development of stem form. *Can. J. For. Res.* **11**, 459–464 (1981).
- Rogers, R. & Hincley, T. M. Foliar weight and area related to current sapwood area in oak. *Forest Sci.* **25**, 298–303 (1979).
- Niklas, K. J. Size-dependent allometry of tree height, diameter and trunk taper. *Ann. Bot.* **75**, 217–227 (1995).
- Tyree, M. T. & Alexander, J. D. Hydraulic conductivity of branch junctions in three temperate tree species. *Trees* **7**, 156–159 (1993).
- Tyree, M. T., Graham, M. E. D., Cooper, K. E. & Bazos, L. J. The hydraulic architecture of *Thuja occidentalis*. *Can. J. Bot.* **61**, 2105–2111 (1983).
- Fitter, A. H. & Strickland, T. R. Fractal characterization of root system architecture. *Funct. Ecol.* **6**, 632–635 (1992).
- Morse, D. R., Lawton, J. H., Dodson, J. H. & Williamson, M. M. Fractal dimension of vegetation and the distribution of arthropod body lengths. *Nature* **314**, 731–733 (1985).
- McMahon, T. A. & Kronauer, R. E. Tree structures: deducing the principle of mechanical design. *J. Theor. Biol.* **59**, 443–436 (1976).
- Enquist, B. J., Brown, J. H. & West, G. B. Allometric scaling of plant energetics and population density. *Nature* **395**, 163–165 (1998).
- Turcotte, D. L., Pelletier, J. D. & Newman, W. I. Networks with side branching in biology. *J. Theor. Biol.* **193**, 577–592 (1998).

Acknowledgements. We thank K. Niklas and M. Tyree for comments. J.H.B. was supported by the NSF, B.J.E. by the NSF and with an NSF post-doctoral fellowship, and G.B.W. by the US Department of Energy. We also thank the Thaw Charitable Trust for support.

Correspondence and requests for materials should be addressed to B.J.E. (e-mail: benquist@unm.edu).

Dynamics of disease resistance polymorphism at the *Rpm1* locus of *Arabidopsis*

Eli A. Stahl*, Greg Dwyer†, Rodney Mauricio†, Martin Kreitman*† & Joy Bergelson*†

*Committee on Genetics, †Department of Ecology and Evolution, University of Chicago, Chicago, Illinois 60637, USA

The co-evolutionary ‘arms race’¹ is a widely accepted model for the evolution of host–pathogen interactions. This model predicts that variation for disease resistance will be transient, and that host populations generally will be monomorphic at disease-resistance (*R*-gene) loci. However, plant populations show considerable polymorphism at *R*-gene loci involved in pathogen recognition². Here we have tested the arms-race model in *Arabidopsis thaliana* by analysing sequences flanking *Rpm1*, a gene conferring the ability to recognize *Pseudomonas* pathogens carrying *AvrRpm1* or *AvrB* (ref. 3). We reject the arms-race hypothesis: resistance and susceptibility alleles at this locus have co-existed for millions of years. To account for the age of alleles and the relative levels of polymorphism within allelic classes, we use coalescence theory to model the long-term accumulation of nucleotide polymorphism in the context of the short-term ecological dynamics of disease resistance. This analysis supports a ‘trench warfare’ hypothesis, in which advances and retreats of resistance-allele frequency maintain variation for disease resistance as a dynamic polymorphism^{4,5}.

Arabidopsis thaliana exhibits a disease-resistance polymorphism in which susceptible individuals are completely lacking *Rpm1* (refs 3, 6). The presence of *Rpm1* homologues in *Brassica*⁶ and the closely